Strain-based risk fracture evaluation with freely available HBMs – A comparison against reference PMHS tests

Vishnuvel Kannan, Felix Ressi, Corina Klug

Abstract Accurate rib fracture prediction is crucial for assessing thoracic injury severity in vehicle crashes. This study compares strain-based rib fracture predictions between THUMS v7.1 and VIVA+ v2.0.0 50M against post-mortem human subject (PMHS) data. PMHS ages were incorporated as covariates in injury risk functions (IRFs). Four load cases—denuded thoracic compression, frontal and lateral hub impacts, and a full-scale frontal sled test—were analysed using HBM for virtual testing (HBM4VT) simulation protocols. Both models generally predicted the risk of three or more fractured ribs (NFR 3+), though underprediction was more common. THUMS showed a stiffer mid-thoracic response in denuded compression due to its larger rib cross-sections. In hub impacts, THUMS' greater cartilage volume led to higher energy absorption and less energy transfer to the ribs. Differences in rib fracture predictions and sensitivity to posture were observed in frontal sled tests. Systematic differences in rib-cage geometry and strain distribution – such as variations in energy transfer and the current exclusion of cartilage from evaluation, were identified as major contributors to model discrepancies. These findings highlight the importance of harmonizing cartilage modelling and improving positioning procedures to enable comparable rib fracture predictions across HBMs for standardized virtual testing.

Keywords HBM4VT, PMHS, rib fracture prediction, THUMS, VIVA+.

I. INTRODUCTION

Rib fractures are common thoracic injuries linked to increased morbidity and fatality in automotive crashes, serving as critical markers of injury severity [1-3]. Accurate predictions of rib fractures are crucial for assessing occupant safety and developing effective restraint systems. Human body models (HBMs), which represent real human anatomy, have emerged as powerful computational alternatives to traditional anthropomorphic test devices (ATDs) for assessing injury severity in vehicle crashes.

Strain-based probabilistic methods have been proposed and widely used to predict rib fractures in HBMs. These methods estimate the fracture probability by mapping the local strains observed in HBM ribs to an injury risk function (IRF), which are developed based on the ultimate strain values derived from experimental tests. One such framework was developed by [4], taking age-adjusted strain thresholds to account for population diversity and utilising a binomial model to predict risk of specific number of ribs. However, this framework had a disadvantage in that it would predict higher injury risk for younger occupants, as only few sample age groups were used in injury risk function (IRF) construction. To address these limitations, the injury risk curve was revised by [5], covering a wide range of ages, which is currently employed by most of the HBMs for rib fracture prediction. Furthermore, a method was introduced by [6] to tune and calibrate the IRFs to achieve a consistent rib fracture prediction between HBMs of different constructions.

Despite these advancements, comparisons to field data often show an overprediction of the rib fracture risk. A study by showed that the SAFER HBM overpredicted the risk of two or more fractured ribs (NFR 2+) when compared to the NASS data [7]. One possible explanation by the authors for this discrepancy was the underestimation of actual fractured ribs in accident databases when CT-scans were used for diagnosis.

Discrepancy of rib fractures can still occur even when HBM ribcage geometry and material properties are age-matched to PMHS. For example, [8] reported an underprediction with the GHBMC thorax model morphed to represent 30- and 70-year-old subjects, attributing it to unaccounted age-related soft tissue differences.

When compared to PMHS tests, uncertainties in boundary conditions remain which could also cause rib

V. Kannan (e-mail: vishnuvel.kannan@tugraz.at) is a PhD student and Research Assistant, F. Ressi is a Senior Researcher, and C. Klug is Associate Professor at the Vehicle Safety Institute, Graz University of Technology, Austria.

fraction prediction differences. Rib fracture prediction can be sensitive to the coefficient of friction values used between the impactor and the HBM, based on a denuded thorax compression test conducted by [7]. Three coefficient of friction values – 0.05, 0.3 and 0.6 – were used and results revealed that approximately a 30% risk difference of NFR 2+ can be expected for a friction value of 0.05 and 0.6. [7].

Postural differences between the PMHS and HBMs could also result in variations in rib fracture predictions. The GHBMC model experienced higher number of fractured ribs when the arms were raised to match the PMHS posture in a hub impact. [9].

Furthermore, geometric variations in ribcage could be an important factor in rib fracture prediction variability. A study was conducted by [10] to find the most influential parameters on rib fracture prediction variability by parameterising the SAFER HBM to evaluate two or more fractured ribs (number of fractured ribs (NFR) 2+) in frontal and near-side impacts. It was found that rib cortical bone thickness, cortical bone material properties, and the rib cross-sectional width had the greatest influence on the rib fracture prediction. Their study also concluded that neither the global rib-cage shape nor the soft tissues covering the rib cage influenced the rib fracture prediction. [10].

The average and standard deviations in cross-sectional properties (total area, cortical bone area, endosteal area and inertial moments) of ribs from 2 to 11, of 240 adults aged between 18 years and 90 years, were compared to six HBMs by [11]. It was found that five out of six HBMs had rib cross-sectional areas that were excessively large along significant portions of most ribs compared to average population corridors. The primary inertial moment (IMAX) and secondary inertial moment (IMIN) remained larger for the THUMS 50M when compared to the VIVA+ 50M, and the male population average. It was also reported that HBM rib cross-section tends to be rounder and larger towards the ends of the sternum. Due to these rib cross-sectional variations across different HBMs, they may exhibit different rib strains even for the same loading conditions, which will affect the rib fracture prediction [11]. It has to be mentioned, however, that the authors of that study [11] assumed a constant thickness of the rib cortical bone for VIVA+ and THUMS, which is not the case in the current versions.

Although all HBMs are validated with PMHS tests, the same test set-ups are not used, and even when this is the case and set-ups are standardised, boundary conditions and results have been interpreted in different ways. Maintaining a consistent simulation set-up is pivotal to compare the injury outcomes of different HBMs. Within the HBM for virtual testing (HBM4VT) framework, standardised load cases for evaluating HBMs neutrally across different loading conditions, representing PMHS tests available in the literature, have been developed [12-13]. By harmonising set-ups using simplified positioning strategies and computational efficiency, HBM4VT aims to qualify HBMs for virtual vehicle crash applications [14]. It also ensures that the initial model itself remains the same in all simulation to enable traceability and avoid that the model could be tuned in between load cases. This means that the repositioning, settling and loading happens at one stage, which is why changes to the vertebrae orientations and isolation of body parts is avoided. For example, in the denuded thorax compression test [15], both the spine positioning or removal of soft tissues are avoided. Instead, HBMs are positioned based on the sternal angle and the hub contact with soft tissues is skipped to represent the denuded thorax. In the frontal sled test [16], HBM torsos are only positioned to match the sternal angle of PMHS. This raises the question about the effect of the introduced simplifications.

Euro NCAP plans to use HBMs alongside ATDs for occupant safety assessment, with an emphasis on robustness. Reliable virtual testing requires consistency across HBMs and solvers, supported by qualification procedures and a clear understanding of discrepancies in rib fracture predictions. Although there are methods like [6] to achieve harmonized rib fracture predictions, the root causes of rib fracture prediction differences between different HBMs remain underexplored.

The objective of this study is to compare the rib fracture predictability of two publicly available HBMs – THUMS v7.1 50M [17] and VIVA+ v2.0.0 50M [18] – by comparing their kinematics and rib fracture predictions with each other and with PMHS test data in four load cases. It seeks to identify differences in rib fracture predictions, analyse rib strain distributions in relation to experimentally observed fracture locations, and explore potential causes of rib fracture prediction discrepancies.

II. METHODS

Two HBMs, THUMS v7.1 50M and VIVA+ v2.0.0 50M, were selected to investigate thoracic loading due to their open-access availability and growing adoption in research. These models were used to investigate thoracic loading and rib fracture risk across four distinct load cases, each representing varying levels of complexity in impact conditions, from localised force application to full-body dynamic loading.

Probabilistic rib injury risk functions (IRFs) were used to quantify the number of fractured ribs (NFR), incorporating the ages of PMHS as covariates. Additionally, the rib strain distributions and the probability of fracture risk for individual ribs were compared to PMHS fracture sites. Statistical comparisons were done to assess each HBM's performance in rib fracture prediction.

Denuded thorax – compression tests

The denuded thorax compression test was chosen to investigate the intrinsic properties of the rib cage itself, eliminating the effects of soft tissue interaction. The thorax was loaded at three anatomical locations – sternum at rib 5 (mid thorax); costal cartilage junction on left rib 3 (upper thorax); and costal cartilage junction on right rib 3 (lower thorax). The indenter velocity was set to 1 m/s with a maximum displacement of 80 mm, matching the experimental set-up of [19]. Two simulation set-ups were carried out for both the HBMs – one with the thoracic soft tissue removal and spine positioning that represents the actual experimental set-up of [19], the other without soft tissue removal (skipping the contact between the indenter and the thoracic soft tissues) and without spine positioning (sternum positioned parallel) representing the HBM4VT set-up [15], as seen in Fig. 1. A sensitive study was also conducted by varying the co-efficient of friction between the indenter and the denuded thorax similar to [7]. Base simulations were performed with a friction value of 0.2, which was increased to 0.6 for comparison.

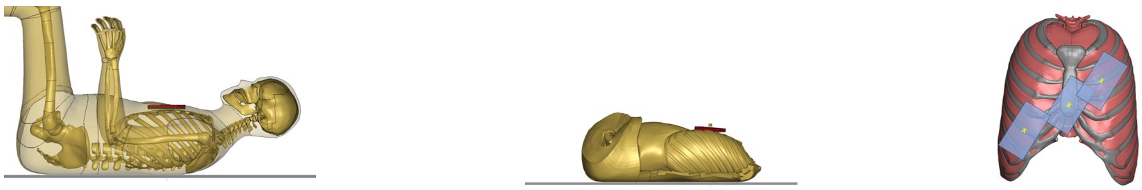

Fig. 1. Impacts to the denuded thorax. *Left*: VIVA+ positioned based on HBM4VT set-up (thoracic soft tissues contact skipped, spine not positioned) [15]; *middle*: VIVA+ denuded thorax positioned based on [19]; *right:* three impact locations on the thorax – upper thorax, mid thorax and lower thorax.

Frontal hub impacts on the complete thorax

In order to assess the influence of thoracic soft tissues, sternum and the costal cartilage on the rib fracture prediction, a frontal hub impact was carried out. The simulation setup was adopted from HBM4VT [20], which represents the frontal hub impact tests performed by [21]. A rigid hub of mass 23.4 kg with an impacting velocity of 6.7 m/s (high speed) was used to strike the thorax at the centre of the sternum at the 4th rib interspace, as shown in Fig. 2. This load case would be used to evaluate the overall stiffness of the rib cage across the HBMs and the energy/strain distribution on the ribs due to the outward bending of the ribs caused by anterior loading.

Lateral hub impacts on the complete thorax

One more hub impact was carried out on the lateral side of the entire thorax to replicate the lateral hub impacts on PMHS conducted by [22]. This load case was chosen to isolate the effects of sternum and costal cartilage on rib fracture prediction. A 23.4 kg impactor was used to strike the thorax laterally at the xiphoid process level, with an impact angle of 30°, see Fig. 2., and velocities ranging from 3.6 m/s to 10.2 m/s [22]. For this study, two impact velocities of 6.5 m/s (medium speed) and 9.5 m/s (high speed) were chosen. The 6.5 m/s case showed moderate number of fractures, while the 9.5 m/s case resulted in a higher number of fractures in the experiment. This selection allowed for evaluation of the HBMs performance across a range of impact severities. The entire simulation set-up was adopted from HBM4VT [23]. Using this load case, the inward bending of the ribs and stiffness of the thorax occurring due to the lateral loading could be evaluated.

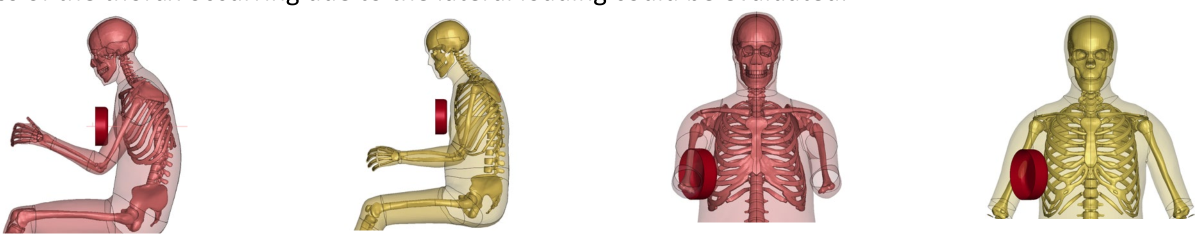

Fig. 2. Frontal and lateral hub impacts on the entire thorax. From left to right: frontal impact on THUMS, frontal impact on VIVA+, lateral impact on THUMS, and lateral impact on VIVA+.

Full-scale frontal sled test

To evaluate rib fracture risks under complex loading, full-scale frontal sled tests conducted on elderly PMHS by [24] were considered. The sled set-up was designed to replicate the seating position of a front-seat passenger, subjected to a frontal impact with a velocity change (ΔV) of 35 km/h. Two restraint conditions, *RCa* and *RCb*, varying the restraint parameters, were applied during the experiment. Due to the extensive fractures observed in PMHS under *RCa*, this restraint configuration was selected for this study. The shoulder-belt load limiter was kept at 2.5 kN and the airbag pressure was maintained at 16 kPa. In the base simulations, using the set-up from HBM4VT [16], the torso of the two HBMs was positioned to match the sternum angle of 24.2^{o} of the PMHS without positioning the spine. This resulted in THUMS sitting in a more reclined posture than VIVA+, as seen in Fig. 3., and also deviating from the actual PMHS posture. To investigate the influence of sternum and spine alignment on rib fracture predictions, additional simulations were conducted: one with both HBMs in their default postures (without any repositioning), and another with the VIVA+ model adjusted to match the default sternum angle of THUMS. These variations enabled a systematic assessment of how postural differences between HBMs and PMHS affect rib fracture risk predictions.

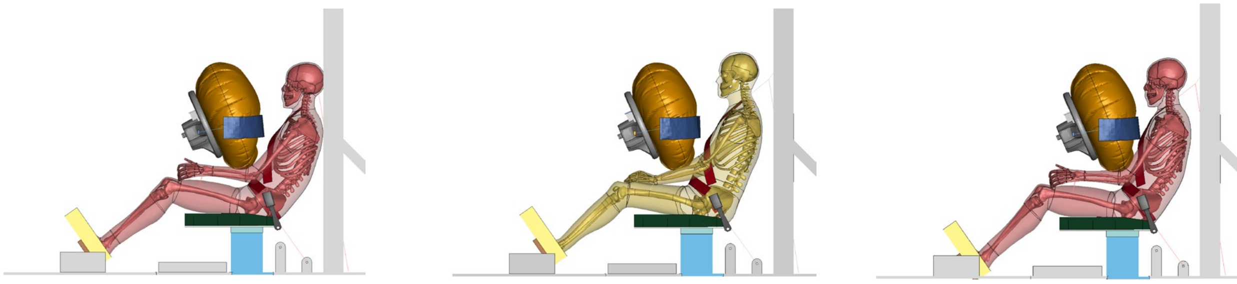

Fig. 3. Full-scale frontal sled test. *Left and middle:* resulting THUMS and VIVA+ postures when positioned based on PMHS sternum angle, respectively; *right:* THUMS default torso posture deviating the PMHS sternal angle.

Probabilistic strain-based rib fracture prediction

The maximum principal strains (MPS) from the maximum integration point of each shell element in every cortical rib of both HBMs were extracted using the Dynasaur library [25]. These strain values were then utilised in the local strain-based IRF developed by Larsson *et al*. [8], to estimate the probability of fracture in each rib. To predict the likelihood of a specific NFR, a generalised binomial model was utilised. The respective PMHS ages for each load case were incorporated as covariates in the IRF, ensuring age-dependent risk estimation. Table AI in Appendix A details the PMHS ages used in each load case. Additionally, contour plots illustrating the MPS distribution across cortical ribs were generated and compared directly with PMHS fracture sites to understand the loading patterns across the ribs. The probability of individual rib fractures for both HBMs, along with MPS distribution and corresponding PMHS fracture sites for all load cases, is comprehensively detailed in Table FI of Appendix F.

Statistical analyses

To quantify and compare the rib fracture prediction performance of THUMS and VIVA+ against the ground truth PMHS rib fractures, statistical analyses were performed. For each matched PMHS – HBM case, the NFR 3+ risk errors were calculated. Additionally, Brier scores were computed to assess probabilistic prediction accuracy. The Brier score is defined as:

$$Brier\ score = \frac{1}{N}\sum_{i=1}^{N}(p_i - o_i)^2$$

where p_i is the predicted probability of rib fracture risk for the i^{th} rib, o_i is the actual fracture outcome (binary; 0 = no fracture, 1 = fracture), and N is the total number of ribs assessed. Predictions were grouped by rib sides (left and right) for both the HBMs. The score reflects how closely each model's risk prediction align with the binary PMHS fracture observations. Lower value indicates a better predictive performance across the load cases.

To further evaluate the model's ability to predict fractures at the individual rib level, mean prediction errors were computed. For each PMHS age, the prediction error was defined as the difference between the HBM's predicted fracture risk and the actual PMHS fracture outcome for each rib. These errors were then averaged across all PMHS ages for each rib and load case. Errors ranging within -0.1 to 0.1 were considered well predicted.

III. RESULTS

Denuded thorax – compression test

The force-deflection responses of both THUMS and VIVA+ were consistent with PMHS data for upper and lower thorax compression tests. However, THUMS produced a significantly stiffer response in the mid-thorax, with forces 15 kN higher than those observed in PMHS and VIVA+ responses. In the HBM4VT set-up, with the intact thoracic soft tissue without spine repositioning, force levels increased by 12–16% compared to the denuded, repositioned configuration, as shown in Fig. B1, Appendix B.

For the prediction of NFR 3+, the THUMS v7.1 model consistently predicted higher fracture probabilities compared to the VIVA+ model, with large differences in the mid thorax region, particularly at ages 52 and 67. Both models, however, converged on high fracture probabilities for older subjects in the lower thorax at age 72 and in the upper thorax at age 75, as seen in Fig. 4. In the NFR 3+ plots, an asterisk (*) indicates PMHS cases with fewer than three fractured ribs, while unmarked cases represent three or more fractured ribs. In the individual rib fracture probability plots, ribs with a box around them indicate fractures observed in the PMHS. These conventions are used consistently throughout the study.

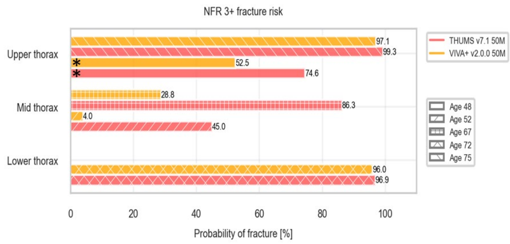

Fig. 4. NFR 3+ fracture risk comparison between THUMS and VIVA+ using the actual set-up with a friction value of 0.2 at three impact locations for different PMHS ages.

Within the HBM4VT approach, VIVA+ and THUMS exhibited diverge fracture risk predictions from the actual set-up: upper thorax impacts had a general 17% higher NFR 3+ risk at age 48, while lower thorax impacts had an 8–11% lower risk. Mid-thorax predictions differed with THUMS 11% lower risk and VIVA+ 6% higher risk at age 67 (see Appendix B, Fig. B2). Increasing the friction coefficient to 0.6 elevated NFR 3+ risk by 32% (upper thorax) and 40% (mid-thorax), while lower thorax predictions were friction insensitive, as shown in Appendix B, Fig. B3.

In the upper thoracic impact, the indenter penetrated the rib cage at the point of loading in tests with PMHS. The 75-year-old PMHS sustained fractures of the costal cartilage, left ribs L2-L6, and right ribs R6-R8, while the 48-year-old PMHS sustained fractures of the cartilage and ribs L2 and L3. Both HBMs performed equally well to each other for the prediction of fracture in ribs L3 and L4. Nevertheless, VIVA+ continued to underpredict fracture in L2, while THUMS underpredicted fracture on L5. PMHS fractures tended to occur near the costal cartilage junction, while HBM fractures occurred at the point of maximum rib curvature, see Fig. 5., and Table FI in Appendix F.

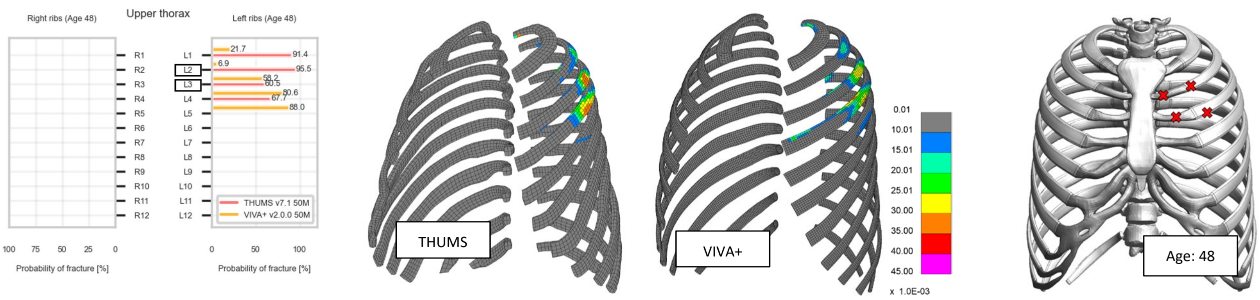

Fig. 5. Denuded thorax (upper impact) – individual rib fractures. *Left*: individual rib fracture risk of THUMS and VIVA+ for age 48 compared to fractures reported in PMHS tests (indicated with box). *Middle:* MPS distribution of both HBMs. *Right*: fracture sites of PMHS aged 48 based on [19].

For mid-thoracic impact, both the 52- and 67-year-old PMHS showed cartilage fracture and over 10 symmetrical cortical rib fractures. THUMS strain distributions remained closer to the PMHS fracture sites, whereas VIVA+ showed more pronounced strain distribution only on the left ribs, deviating from the PMHS. Both HBMs computed higher fracture probabilities on the left rib L1 than PMHS. Severe differences between ribs L3 and L4 were noted, such that THUMS predicted 57.8% fracture of L4 and 10.8% fracture of VIVA+, whereas VIVA+ predicted 79% fracture of L3 and 3.4% fracture of THUMS. Both the models underpredicted overall rib fractures compared to PMHS.

For lower thoracic impact, both HBMs consistently predicted fractures of right ribs R4-R7 and none of left ribs. However, PMHS exhibited fractures on both sides of the rib cage: right ribs (R2-R5, R7, and R8) and left ribs (L2-L4, L6-L8), including cartilage. The two HBMs predicted fracture patterns of ribs matched better with PMHS fracture sites.

Frontal hub impacts on the complete thorax

In the frontal hub impact tests, the THUMS thorax demonstrated approximately 12% greater stiffness compared to VIVA+, as seen in Fig. C1, Appendix C. Despite this increased stiffness, THUMS predicted only 4.4% NFR 3+, while VIVA+ predicted a much higher risk of 99.3% for an 80-year-old. The corresponding PMHS aged 80 sustained 13 fractured ribs. Similarly, for a 72-year-old, VIVA+ predicted an NFR 3+ risk of 94.4%, whereas THUMS predicted only 1.2%. The PMHS aged 72 suffered 17 fractured ribs. For the PMHS of age 29 years, no fractures were reported in the experimental tests. But THUMS predicted an 85.4% risk and VIVA+ predicted a 36.7% risk for one or more fractured ribs, see Fig. C2, Appendix C.

Huge variations were seen between both the HBMs in predicting individual rib fracture risk. VIVA+ demonstrated a very good prediction of fractures of left (L3-L6) and right ribs (R3-R6), aligning well with PMHS aged 80 and 72. However, it overpredicted fractures for ribs L1 and R1, Fig. 6. The strain distribution in VIVA+ remained nearly symmetrical across both sides of the rib cage. By comparison, THUMS showed higher strain value and fracture at L1 across all ages and at L7, which were not observed in any of the PMHS.

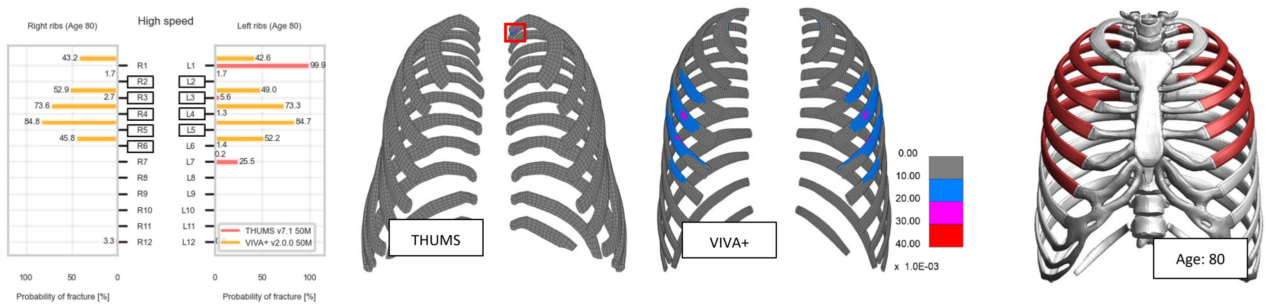

Fig. 6. Frontal hub impacts – individual rib fractures. *Left*: predicted individual rib fracture risk of THUMS and VIVA+ for age 80. *Middle:* MPS distribution of both HBMs' cortical ribs. *Right*: fractures observed in PMHS (in red) of 80-year-old based on [21].

Lateral hub impacts on the complete thorax

In both the medium and high-speed impacts, THUMS showed a slightly greater thoracic stiffness compared to VIVA+ (refer see Appendix D, Fig. D1). All the tested PMHS showed NFR 3+ rib fractures. In medium-speed impact, VIVA+ showed only 29% risk of NFR 3+, while THUMS showed a greater risk of 78% for PMHS aged 38. For older PMHS ages (64, 66), both models showed consistently high risks ranging from 92% to 100%.

In the high-speed impact, both models predicted similarly high NFR 3+ fracture risks (91%–100%) for PMHS aged 29, 49, and 64 years. However, a notable difference emerged in predicting NFR 7+ fractures for the 64-year-old PMHS, which sustained 13 fractured ribs in experimental tests. VIVA+ predicted a 70.8% risk of NFR 7+ fractures, while THUMS predicted only 27.8%, indicating significant variability between the models, see Fig. D2, Appendix D.

This discrepancy is further illustrated in Fig. 7, where VIVA+ displayed strain over a larger area, including the opposite side of the rib cage. In contrast, THUMS exhibited very high strain values on the striking side, with minimal strains observed on the opposite side.

Regarding individual rib fractures, the 64-year-old PMHS sustained fractures in right ribs (R2-R8) and left ribs (L4-L8). Both HBMs accurately predicted fractures of right ribs (R3-R8), with VIVA+ demonstrating a 51% higher risk of R3 fracture than THUMS, which aligned well with PMHS data, Fig. 8. However, despite VIVA+ indicating strains on the opposite side of the rib cage, it only predicted a lower fracture risk and did not accurately replicate the PMHS fracture pattern. Detailed rib fracture prediction comparisons for other ages (29, 49 years) are listed in Appendix F, Table FI.

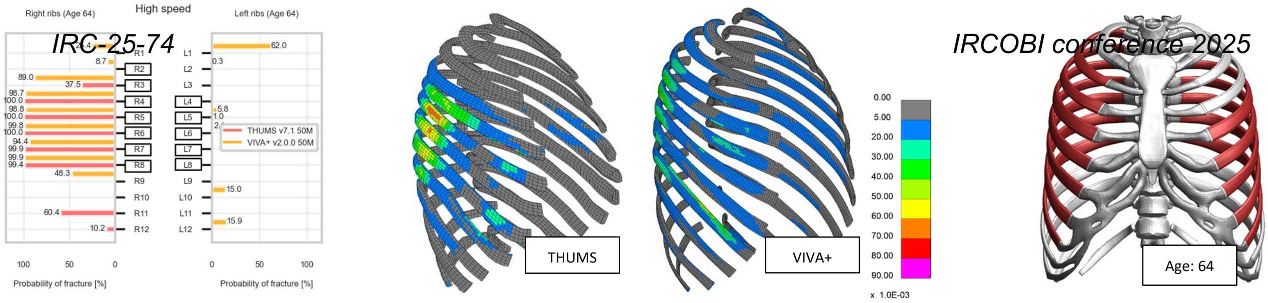

Fig. 7. Lateral hub impacts – individual rib fractures. *Left*: predicted individual rib fracture risk of THUMS and VIVA+ for age 64. *Middle:* MPS distribution of both HBMs' cortical ribs. *Right*: fractures observed in PMHS (in red) of 64-year-old based on [22].

Full-scale frontal sled test

In full-scale frontal sled tests using the HBM4VT set-up, both HBMs showed similar pelvis and T8 x-displacement, aligning well with the PMHS data. However, head and T1 x-displacement were overestimated. When the HBMs were positioned in their default torso posture, VIVA+ demonstrated good agreement with PMHS kinematics, while THUMS exhibited noticeable differences in T8, T1, and head displacements, as shown in Appendix E, Fig. E1.

In predicting NFR 3+ risk, both HBMs showed similar results of approximately 90–95% for age 94, while VIVA+ demonstrated lower risks than THUMS for other ages (68, 74 years) when using the HBM4VT set-up. However, when positioned in the default torso posture, the risk dropped significantly for the THUMS model, whereas the VIVA+ model remained unaffected. Additionally, VIVA+ continued to show similar rib fracture risk even when its sternum angle was matched to the default sternum angle of THUMS. (Fig. 8).

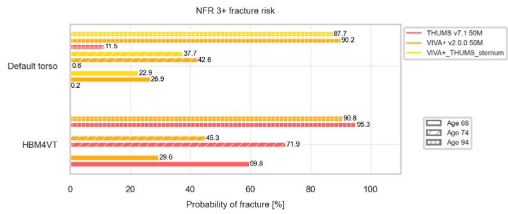

Fig. 8. NFR 3+ fracture risk comparison for THUMS and VIVA+ HBMs under HBM4VT and default torso, and for VIVA+ with the THUMS default sternum posture (yellow bars) for PMHS aged 68, 74, and 94 years.

A greater difference was observed between the two HBMs in predicting individual rib fracture risks. As seen in Fig. 9, for the 68-year-old THUMS predicted higher fracture risks at ribs L7 (85.4%), L6 (23.1%), and R11 (96.9%), primarily occurring during the unloading phase. In contrast, VIVA+ showed higher fracture risks at left rib L1 (92.4%) and right rib R1 (67.9%). Although VIVA+ predicted lower fracture risks for the remaining ribs compared to THUMS, its strain distribution across the entire rib cage closely matched the fractured ribs/sites observed in PMHS aged 68 and 74 years. THUMS, however, failed to accurately depict strain distribution across the rib cage, with strains remaining concentrated at higher values (0.025–0.035). A 94-year-old PMHS exhibited rib fractures near the costovertebral end, which was not predicted by either of the HBMs.

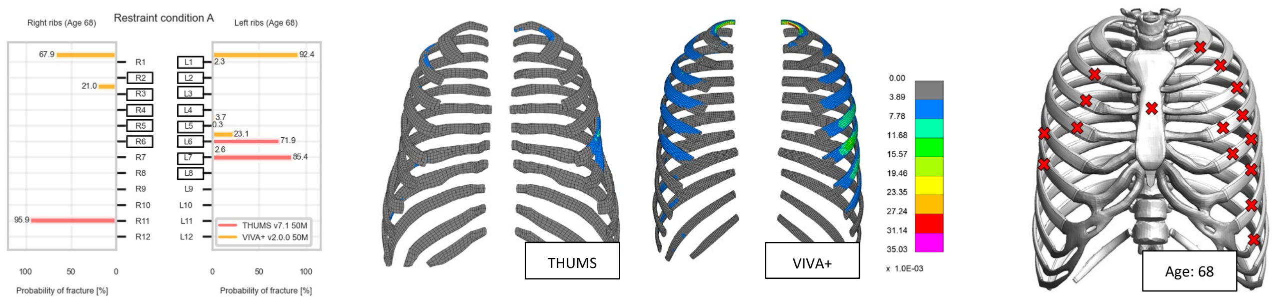

Fig. 9. Frontal sled test – individual rib fractures. *Left*: individual rib fracture risk of both HBMs for age 68. *Middle:* MPS distribution of both HBMs' cortical ribs at 100 ms. *Right*: fracture sites of PMHS aged 68 [24].

Statistical analyses

Table GI compares NFR 3+ risk errors by THUMS and VIVA+ across load cases for different PMHS ages. Both models agreed well with PMHS in lower thorax compression and high-speed lateral impacts. THUMS underpredicted risks in frontal hub impacts (absolute difference ≥0.9), while VIVA+ closely matched PMHS (absolute difference <0.1). VIVA+ showed large deviations in mid-thorax compression. In full-scale frontal sled tests, both models underpredicted risks in older subjects, with THUMS generally closer than VIVA+.

Table GIII presents Brier scores for rib fracture predictions, colour-coded from green (≤0.1, best) to red (>0.5, poor). Both models performed well in upper thorax compression and medium-speed lateral hub impacts (≤0.18). Prediction quality declined in mid-thorax compression (up to 0.51 for VIVA+ right ribs, 0.47 for THUMS left ribs) and high-speed lateral hub impacts (0.38–0.40 for left ribs). In frontal hub impacts, VIVA+ scored well (0.10), while THUMS showed higher errors (0.27–0.32). The poorest predictions occurred in the frontal sled test (≥0.5 for THUMS, ≥0.4 for VIVA+).

Fig. G1 provides a detailed rib-by-rib heatmap of mean prediction errors for THUMS and VIVA+ across all load cases. Ribs with a mean prediction error outside the range of -0.1 to 0.1 are marked with an "x", indicating poor performance. The overall percentage of underpredicted ribs (blue), correctly predicted ribs (green), and overpredicted ribs (red) for each HBM per load case is summarized in Fig. 10. In the denuded thorax compression and frontal sled test cases, underprediction (over 58%) was most common for both HBMs. Correct predictions were highest in the frontal hub impact, with VIVA+ at 62.5% and THUMS at 50%. Overprediction was consistently low, peaking at 16.7% in the lateral hub impact for both HBMs. Overall, underpredictions remained as the dominant trend for both the HBMs.

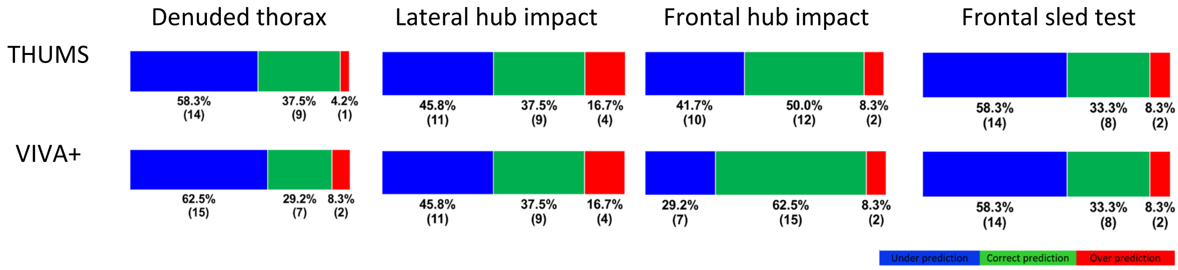

Fig. 10. Overall percentage of underpredicted ribs (blue), correctly predicted ribs (green), and overpredicted ribs (red) for each HBM per load case. The values below the percentages represent the number of ribs.

IV. DISCUSSION

This study evaluated the rib fracture prediction capabilities of two openly available HBMs—THUMS v7.1 50M and VIVA+ v2.0.0—across four distinct load cases. Both HBMs demonstrated reasonably close NFR 3+ risk predictions to PMHS outcomes in the lateral hub impacts. For the frontal hub impact, severe underprediction was demonstrated by the THUMS. Both models remained underpredicted for NFR 3+ risk in the full-scale frontal sled test. Furthermore, neither HBM was not able to predict the exact number of fractures or replicate the exact fracture patterns observed in PMHS, with underprediction being the predominant trend. The following sections explore potential reasons for these discrepancies in rib fracture outcomes.

Influence of rib geometry and flexural rigidity

Rib cross-sectional geometry is a key factor influencing fracture variability, as noted in [10], and likely plays a similar role in this study. Each rib acts like a beam that exhibits bending resistance or flexural stiffness under loading. This bending resistance is determined by the product of Young's modulus and the second area moment of inertia about the bending axis. While both HBMs have nearly the same Young's modulus of the cortical bone, they differ in rib geometries. THUMS ribs exhibited higher second moments of inertia (IMAX and IMIN) compared to VIVA+ for the lower ribs [11]. This can result in greater bending resistance and overall ribcage stiffness of THUMS. However, the global stiffness played a less significant role in the upper and lower denuded thorax compression tests for both HBMs, where the response is dominated by the localised rib bending. Similarly, in lateral hub impacts, global ribcage stiffness played a reduced role.

Influence of costal cartilage and energy transfer

A recent experimental study [26] has highlighted the significant role of costal cartilage in rib bending properties and fracture mechanics. Ribs with costal cartilage experienced lower force but greater displacement and longer time to fracture compared to isolated ribs. [26].

A crucial role of costal cartilage in load transfer and rib fracture prediction was also identified in our investigations. THUMS costal cartilage appears to act as an energy-absorber during impacts. This was particularly evident in frontal hub impact, as shown in Fig. 11., where THUMS showed minimal energy transfer to cortical ribs leading to rib fracture underprediction.

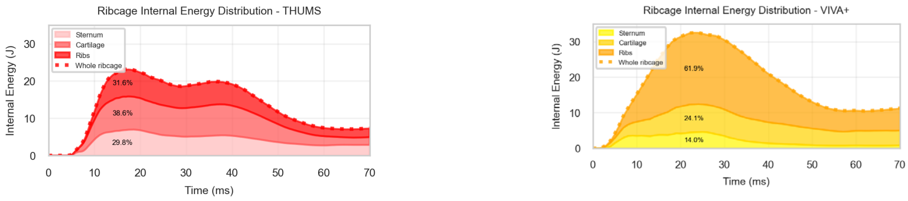

Fig. 11. Rib-cage internal energy distribution for the frontal hub impact. *Left*: ribcage internal energy distribution of THUMS. *Right*: rib-cage internal energy distribution of VIVA+.

Moreover, asymmetric loading was seen with a very high strain value observed only at the vertebral end of left rib L1. In contrast, VIVA+ demonstrated more pronounced load transfer and symmetric loading, aligning better with PMHS fracture patterns. Upon further investigation, it was found that while the material properties of costal cartilage are very similar in both HBMs, their geometrical properties differ. Specifically, THUMS possesses almost 2.5 times greater cartilage volume compared to VIVA+, refer Fig. H1. This increased cartilage volume in THUMS likely contributes to its greater capacity for energy absorption, thereby reducing the energy transferred to the cortical ribs. Moreover, unsymmetrical cartilage volumes – with the right side containing about 500 mm³ more cartilage than the left (Fig. H2.), may explain the observed asymmetric loading.

Lateral hub impacts further emphasised the importance of load distribution across the rib cage. While both models showed good agreement with PMHS fractures on the striking side, VIVA+ showed minimal strains on the other side too, but still underpredicted fractures when compared to PMHS, whereas THUMS showed no fracture risk on the contralateral side at all. This variation may be again related to how each HBM represents the costal cartilage and its role in energy distribution across the ribcage, see Appendix D, Fig. D3. These findings underscore the role of costal cartilage in energy transfer and highlight a potential improvement in HBM development.

Influence of boundary conditions and initial HBM posture

Boundary conditions and initial posture also had a measurable effect on rib fracture prediction. In the denuded thorax compression test, increasing the co-efficient of friction from 0.2 to 0.6, led to a 30–40% increase in NFR 3+ risk, consistent with findings in [7]. One of the objectives of the study was to compare the simple and efficient positioning approach followed in HBM4VT to the actual experimental set-up for the denuded thorax compression test. The HBM4VT set-up, which retained soft tissues and avoided spine repositioning, showed only minimal differences in force-deflection response and rib fracture prediction compared to the denuded, repositioned set-up.

Sled tests revealed that THUMS was more sensitive to small changes of the initial posture than VIVA+. When THUMS was used in its default torso posture without aligning the sternum angle, it underpredicted NFR 3+ risk. In contrast, adjusting THUMS to match the sternum angle (HBM4VT approach) the NFR 3+ risk was elevated. In the HBM4VT approach, the predicted rib fractures by THUMS were L6, L7, and the floating rib R11. But in default posture, THUMS only showed fracture at L7. The floating rib fracture could have resulted from THUMS being positioned slightly reclined. On further investigating, the internal energy distribution throughout the ribcage remained similar between both the approaches, with 16% higher internal energy for the HBM4VT approach as seen in Fig. E2. We had hypothesized that in one load case more energy is transferred through the costal cartilage than in the other, but in fact the main difference was in the sternum itself.

The HBM4VT approach, with aligning sternum angle, seems to be a good pragmatic approach to achieve better alignment with the PMHS kinematics and a more consistent NFR 3+ risk prediction between HBMs with THUMS. VIVA+, on the other hand, consistently predicted NFR 3+ between 88% and 91% for the age 94 across all tested postures, indicating lower sensitivity to positioning.

PMHS variability and outliers in experiments

PMHS, even when tested under controlled conditions exhibit variability in fracture patterns due to inter-subject variability [27]. Previous research has also shown that even among rib samples of similar age, parameters like yield stress and failure strain can vary substantially [28].

For instance, in the lateral high-speed impact test considered, two PMHS of the same age (49 years) sustained markedly different injuries—one had 14 fractured ribs, while the other had only 6.

In the upper denuded thorax compression test, the indenter penetrated the ribcages of subjects 2 and 3. Subject 2 exhibited only two fractured ribs; however, it is likely that more fractures would have occurred had the indenter not breached the ribcage. It was also reported in the full-scale frontal test that PMHS 3 (aged 94) was an outlier, as the PMHS had an overly stiff spine due to the formation of osteophytes and the fractures occurred at the costovertebral junction, which is not a commonly observed fracture pattern [24].

As a result, variability and outliers in PMHS responses can introduce challenges in accurately assessing HBM performance. It is theoretically possible to match HBM predictions to the exact fractures observed in PMHS by modifying the material properties and geometry of the HBMs to a specific PMHS [29-30]. However, the goal of this study was not to achieve such prediction. Instead, we sought to compare the rib fracture predictions of the two models in their original states, using only age as a covariate in the IRF to predict fractures and compare it with PMHS data. This approach allowed us to highlight the inherent variability between models that are readily available and to evaluate the general predictive capabilities of each.

Limitations and future perspectives

There exist several limitations in this study. First, comparison was done with only two HBMs. In future, a larger number of HBMs should be used to quantify variations in rib fracture prediction.

Secondly, uncertainties from boundary conditions have not been quantified, except for the coefficient of friction in the denuded thorax tests. Furthermore, some simplifications in the replication of the PMHS tests were made in the lateral and frontal hub impact tests, the upper arms were not repositioned to correspond with the PMHS posture. If the arms were to be held overhead, the consequent reduction of the thickness of thoracic adipose tissue might have led to decreased energy absorption of soft tissues and the rib fracture risk would have increased, as described in [9].

Thirdly, while the HBMs represent midsized males, the PMHS specimens varied in body weight across load cases. No morphing or anthropometric scaling was applied to the HBMs, which is a significant limitation of our study. Furthermore, PMHS-specific ribcage property data were not available, which was also a constraint in our study. As a result, it was not feasible to directly compare the rib geometry of the HBMs to that of the PMHS. Lastly, the limited PMHS sample size used in the statistical analysis may affect the reliability of the findings.

Finally, the influence of sternum geometry and material properties on rib fracture predictions remains an open question. Two HBMs that differ in terms of geometry and material properties have been compared, which is why no isolated effects could be investigated. Looking at the material data of the costal cartilage, however, only small differences in the material modelling have been observed, which is why the geometry seems to be the main driving force here. In future studies, material properties between the models could be exchanged to investigate effects separately. However, as the two models drastically differ in their modelling strategies, such an approach might not be meaningful.

Given costal cartilage's significant role in thoracic biomechanics, particularly in energy absorption during impact, its lack of validation and calibration data is a key limitation. The current models do not include age-related calcification, which alters cartilage stiffness and influences fracture patterns and which is especially important for the rib fracture predictions of elderly occupants. To enhance rib fracture prediction accuracy, future research should focus on accurate cartilage modelling within HBMs.

V. CONCLUSION

This study compared rib fracture predictions of freely available HBMs using strain-based probabilistic methods with PMHS age-adjusted IRFs across four distinct load cases, all within HBM neutral simulation set-ups. It also analysed the strain distribution of the cortical ribs of the HBMs and compared it with the PMHS fracture sites.

Overall, both HBMs were able to predict NFR 3+ in most of the load cases. In the frontal hub impact, VIVA+ showed prediction closer to the PMHS compared to THUMS. THUMS showed a stiffer response in the mid thorax on the denuded thorax compression test, attributable to the larger cross-sectional cortical rib geometry than VIVA+. In frontal and lateral hub impacts, the larger cartilage volume of THUMS resulted in higher energy absorption, transferring less energy to the cortical ribs and thereby affecting the rib fracture prediction.

In general, both models showed more often an under- than overprediction of NFR 3+. The HBM4VT approach for the denuded thorax tests and positioning in the sled tests proved to be an efficient pragmatic approach. Full-scale frontal sled tests revealed posture sensitivity for THUMS and differences in fracture locations between models. For the prediction of the individual fractured ribs difference between the models and the models to the PMHS increased.

These findings aim to guide the ongoing Euro NCAP efforts to integrate HBMs in vehicle safety assessments. Future work should focus on the validation and harmonisation of the costal cartilage geometry and definition of robust positioning procedure to reach comparable results for rib fracture predictions in virtual testing. However, as these variations might be also present in real humans, restraint systems should be designed in a way to reduce large sensitivities. Additionally, assessment protocols should award the robustness of systems being able to provide protection for occupants with different rib cage geometries.

VI. ACKNOWLEDGEMENTS

The authors gratefully acknowledge the IT Services (ZID) of Graz University of Technology, Austria, for providing access to high-performance computing resources. The authors also acknowledge that the HBM4VT set-ups used within this study were obtained from OpenVT hosted by OVTO.

VII. REFERENCES

[1] Ekambaram, K., Frampton, R., Lenard, J. (2019) Factors associated with chest injuries to front seat occupants in frontal impacts. *Traffic Injury Prevention*, **20**(sup2): pp. S37–S42.

[2] Holcomb, J. B., McMullin, N. R., Kozar, R. A., Lygas, M. H., Moore, F. A. (2003) Morbidity from rib fractures increases after age 45. *Journal of the American College of Surgeons*, **196**(4): pp. 549–555.

[3] Pipkorn, B., Iraeus, J., Lindkvist, M., Puthan, P., Bunketorp, O. (2020) Occupant injuries in light passenger vehicles-A NASS study to enable priorities for development of injury prediction capabilities of human body models. *Accident Analysis& Prevention*, **138**: 105443.

[4] Forman, J. L., Kent, R. W., *et al*. (2012) Predicting rib fracture risk with whole-body finite element models: development and preliminary evaluation of a probabilistic analytical framework. *Annals of Advances in Automotive Medicine*, **56**: pp. 109–124.

[5] Larsson, K.-J., Blennow, A., Iraeus, J., Pipkorn, B., Lubbe, N. (2021) Rib Cortical Bone Fracture Risk as a Function of Age and Rib Strain: Updated Injury Prediction Using Finite Element Human Body Models. *Frontiers in Bioengineering and Biotechnology*, **9**: 677768.

[6] Forman, J., Kulkarni, S., *et al*. (2022) A Method for Thoracic Injury Risk Function Development for Human Body Models. *Proceedings of the IRCOBI Conference*, 2022. Porto, Portugal.

[7] Pipkorn, B., Iraeus, J., Björklund, M., Bunketrop, O., Jakobsson, L. (2019) Multi-Scale Validation of a Rib Fracture Prediction Method for Human Body Models. *Proceedings of the IRCOBI Conference*, 2019, Florence, Italy.

[8] Schoell, S. L., Weaver, A. A., Vavalle, N. A., Stitzel, J. D. (2015) Age- and sex-specific thorax finite element model development and simulation. *Traffic Injury Prevention*, **16**(Suppl 1): pp. S57–S65.

[9] Blade, S., Kleeck III, W. von, *et al*. (2024) Meta-Analysis of Rib Fracture in GHBMC Detailed Human Body Models: A Retrospective Study. *Proceedings of the IRCOBI Conference*, 2024, Stockholm, Sweden.

[10] Larsson, K.-J., Iraeus, J., Holcombe, S., Pipkorn, B. (2023) Influences of human thorax variability on population rib fracture risk prediction using human body models. *Frontiers in Bioengineering and Biotechnology*, **11**: 1154272.

[11] Holcombe, S., Huang, Y. (2023) Cross-sectional properties of rib geometry from an adult population. *Frontiers in Bioengineering and Biotechnology*, **11**: 1158242.

[12] Ressi, F., Schneider, B., *et al*. (2025, In review) Development of a Robust Human Body Model Qualification Methodology: Ensuring Biofidelity for Occupant Protection Assessments in Virtual Testing. *Proceedings of the IRCOBI Conference*, 2025, Vilnius, Lithuania. [in review]

[13] Open Virtual Testing Organisation (OVTO). HBM4VT Validation Catalogue, https://openvt.eu/EuroNCAP/hbm4vt-validation-catalogue. [24.03.2025].

[14] Klug, C., Wernicke P. HBM4VT - Development of a roadmap for the use of human body models in virtual testing. https://projectvirtual.eu/wp-content/uploads/2022/12/HBM4VT_Motivation_Status_Outlook_13092022.pdf. [13.09.2022].

[15] Open Virtual Testing Organisation (OVTO). HBM4VT Validation Catalogue - Shaw_2007, https://openvt.eu/EuroNCAP/hbm4vt-validation-catalogue/ls-dyna/shaw_2007. [25.03.2025].

[16] Open Virtual Testing Organisation (OVTO). HBM4VT Validation Catalogue - Lopez_Valdes_2017, https://openvt.eu/EuroNCAP/hbm4vt-validation-catalogue/ls-dyna/lopez_valdes_2017. [25.03.2025].

[17] Toyota Central R&D Labs. Inc. Total HUman Model for Safety THUMS®. https://www.toyota.co.jp/thums/. [15.02.2025].

[18] John, J., Klug, C., Kranjec, M., Svenning, E., Iraeus, J. (2022) Hello, world! VIVA+: A human body model lineup to evaluate sex-differences in crash protection. *Frontiers in Bioengineering and Biotechnology*, **10**: 918904.

[19] Shaw, G., Lessley, D., Evans, J., Crandall, J., Shin, J.. (2007) Quasi-static and Dynamic Thoracic Loading Tests: Cadaveric Torsos. *Proceedings of the IRCOBI Conference*, 2007, Maastricht, The Netherlands.

[20] Open Virtual Testing Organisation (OVTO). HBM4VT Validation Catalogue - Kroell_1971, https://openvt.eu/EuroNCAP/hbm4vt-validation-catalogue/ls-dyna/kroell_1971. [10.02.2025].

[21] Kroell, C. K., Schneider, D. C., Nahum, A. M. (1971) Impact Tolerance and Response of the Human Thorax. *Proceedings of the 15th Stapp Car Crash Conference*, 1971, California, USA.

[22] Viano, D. C. (1989) Biomechanical Responses and Injuries in Blunt Lateral Impact. *Proceedings of the 33rd Stapp Car Crash Conference*, 1989, Washington D.C., USA.

[23] Open Virtual Testing Organisation (OVTO). HBM4VT Validation Catalogue - Lateral_Impactors_Viano_1989, https://openvt.eu/EuroNCAP/hbm4vt-validation-catalogue/ls-dyna/lateral-impactors-viano-1989. [08.02.2025].

[24] Lopez-Valdes, F. J., Mroz, K., *et al*. (2018) Chest injuries of elderly postmortem human surrogates (PMHSs) under seat belt and airbag loading in frontal sled impacts: Comparison to matching THOR tests. *Traffic Injury Prevention*, **19**(sup2): pp. S55–S63.

[25] Schachner, M., Micorek, J., *et al*. DynaSaur (Dynamic simulation analysis of numerical results). https://gitlab.com/VSI-TUGraz/Dynasaur. [02.07.2024].

[26] Schaffer, R., Kang, Y.-S., *et al*. (2024) Comparison of Bending Properties in Paired Human Ribs with and without Costal Cartilage. *Stapp Car Crash Journal*, **68**: pp. 104–154.

[27] Kent, R. (2008) Frontal thoracic response to dynamic loading: the role of superficial tissues, viscera and the rib cage. *International Journal of Crashworthiness*, **13**(3): pp. 289–300.

[28] Katzenberger, M. J., Albert, D. L., Agnew, A. M., Kemper, A. R. (2020) Effects of sex, age, and two loading rates on the tensile material properties of human rib cortical bone. *Journal of the Mechanical Behavior of Biomedical Materials*, **102**: 103410.

[29] Antona-Makoshi, J., Yamamoto, Y., *et al.* (2015) Age-Dependent Factors Affecting Thoracic Response: A Finite Element Study Focused on Japanese Elderly Occupants. *Traffic Injury Prevention*, **16**(sup1): pp. S66–S74.

[30] Takahira, Y., Akima, S., Kusuhara, Y., Tanase, N., Kitagawa, Y. (2021) Cross-Sectional Analysis of Rib Fracture Mechanism of Elderly Occupant in Frontal Collision using THUMS. *Proceedings of the IRCOBI Conference*, 2021, Online.

VIII. APPENDIX

Appendix A
PMHS data

PMHS and corresponding ages used in IRF for each load case.

TABLE AI
LOAD CASES AND CORRESPONDING PMHS DETAILS USED IN THIS STUDY

Load case	Impact type/Location/Velocity	PMHS ID used in experiment	PMHS - AGE	PMHS – Height (cm)	PMHS – Weight (kg)
Denuded thorax compression [19]	Upper thorax – 1 m/s	Subject 2	75	183	73
		Subject 3	48	168	68
	Mid thorax – 1m/s	Subject 4	52	179	77
		Subject 5	67	170	77
	Lower thorax – 1 m/s	Subject 1	72	180	66
Lateral hub impact [22]	Medium speed – 6.5 m/s	947	38	166.5	56.25
		RNY2	64	171	61.69
		954	66	159	56.25
	High speed – 9.5 m/s	863	49	176	107
		993	49	173	70.76
		986	29	173	70.3
		063	64	173	48.54
Frontal hub impact [21]	High speed – 6.7 m/s	15FM	80	165	53
		20FM	29	180	57
		22FM	72	183	75
Full-scale frontal sled test [24]	Restraint condition A	PMHS 1	74	167	66
		PMHS 2	68	184	76
		PMHS 3	94	156	94

Appendix B
Denuded thorax – compression tests

Force Deflection response – comparison between actual and HBM4VT set-ups for THUMS and VIVA+.

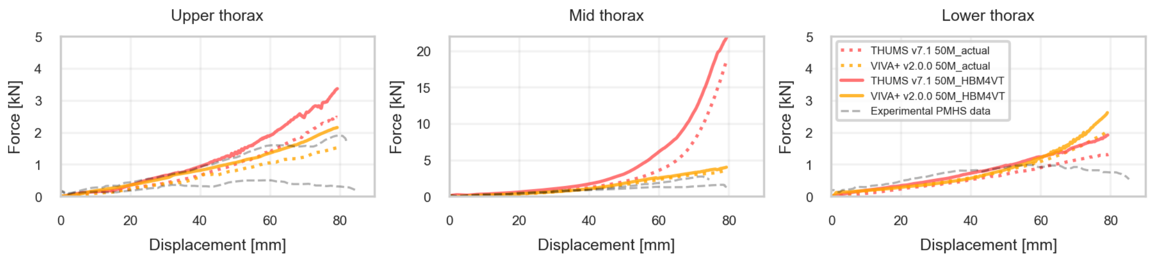

Fig. B1. Comparison of thoracic stiffness of THUMS and VIVA+ positioned based on HBM4VT and actual set-up at upper, mid and lower thorax, respectively.

NFR 2+ and NFR 3+ rib fracture predictions – comparison between actual and HBM4VT set-ups for THUMS and VIVA+.

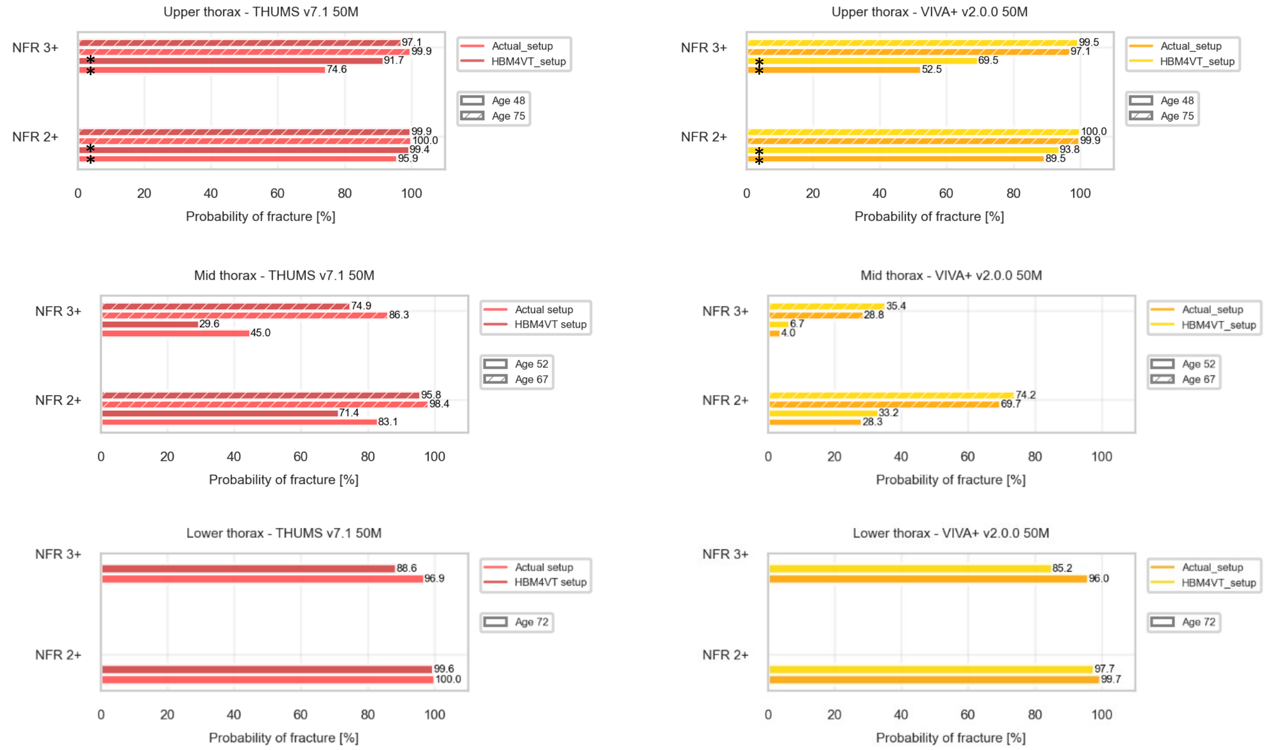

Fig. B2. Comparison of number of fractured ribs of THUMS and VIVA+ positioned based on HBM4VT and actual set-up at upper, mid and lower thorax, respectively.

NFR 2+ and NFR 3+ rib fracture predictions – comparison between different friction values for THUMS and VIVA+.

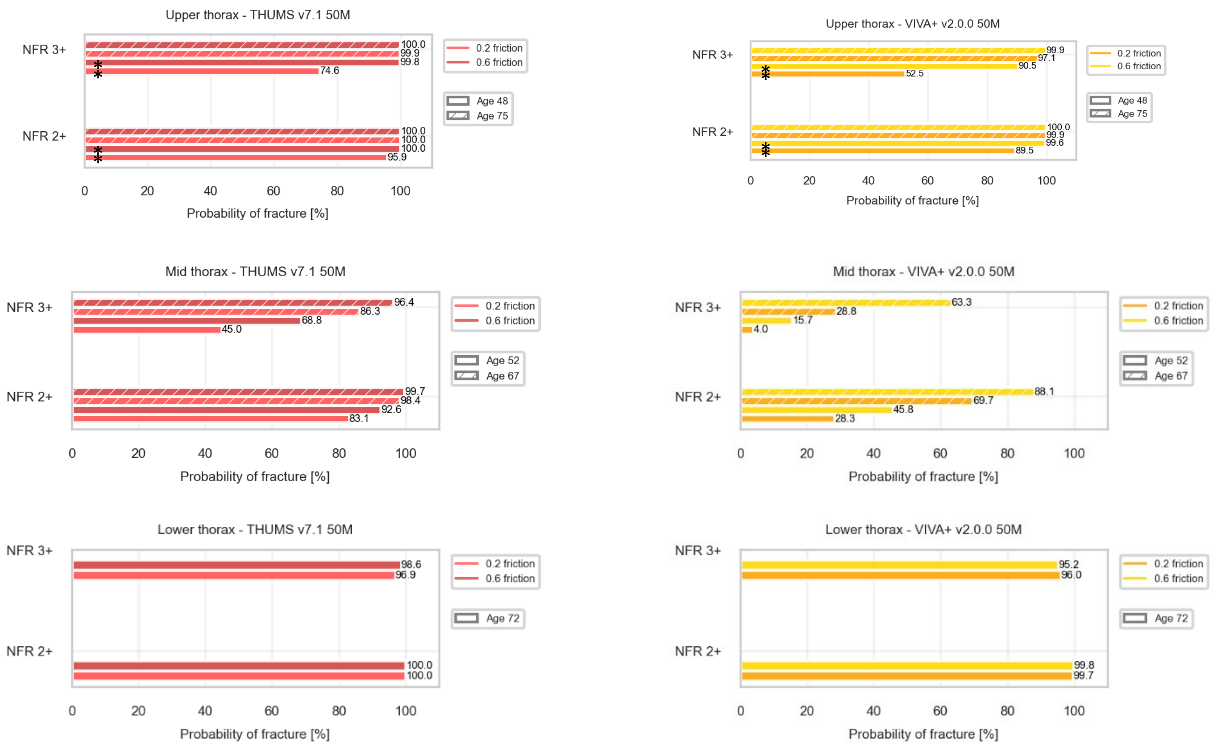

Fig. B3. Comparison of number of fractured ribs of THUMS and VIVA+ for friction values of 0.2 and 0.6 positioned based on actual experimental set-up at upper, mid and lower thorax, respectively.

Appendix C
Frontal hub impact on complete thorax

Force deflection response – comparison between THUMS and VIVA+ with PMHS data.

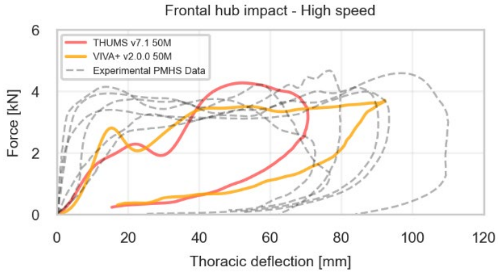

Fig. C1. Comparison of thoracic stiffness response of THUMS and VIVA+ with PMHS data during frontal hub impact at 6.7 m/s.

NFR 1+ and NFR 3+ fracture prediction – comparison between THUMS and VIVA+.

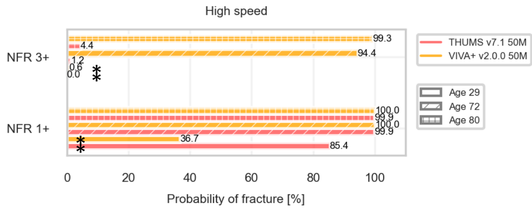

Fig. C2. Comparison of NFR 1+ and NFR 3+ risk predicted by THUMS and VIVA+ for PMHS aged 29, 72, and 80 years in the frontal hub impact.

Appendix D
Lateral hub impact on complete thorax

Force deflection response – comparison between THUMS and VIVA+ with PMHS data.

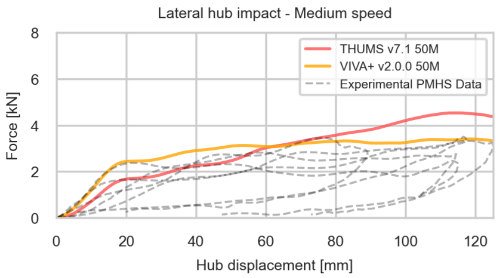

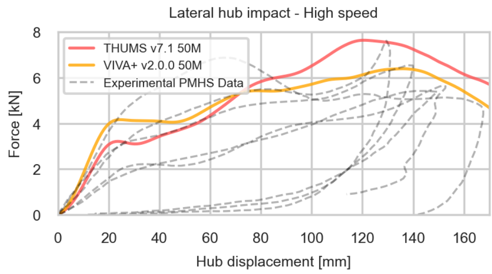

Fig. D1. Comparison of thoracic stiffness response of THUMS and VIVA+ with PMHS data during lateral hub impacts. *Left:* medium speed impact at 6.5 m/s. *Right:* high speed impact at 9.5 m/s.

NFR 3+ and NFR 7+ fracture prediction – comparison between THUMS and VIVA+.

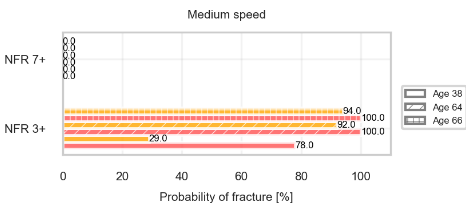

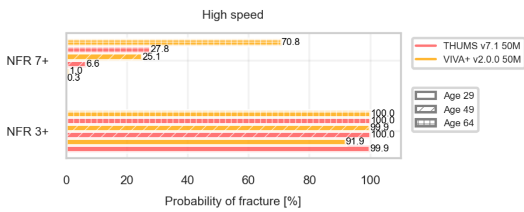

Fig. D2. Comparison of NFR 3+ and NFR 7+ risk predicted by THUMS and VIVA+. *Left*: medium speed impact. *Right*: high speed impact.

Ribcage internal energy distribution – comparison between THUMS and VIVA+.

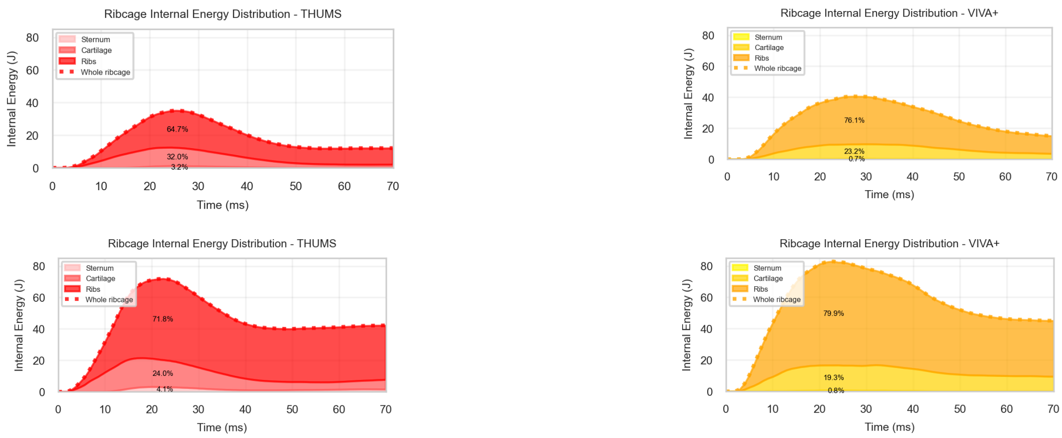

Fig. D3. Rib-cage internal energy distribution for the in lateral hub impacts. *Top left-right*: ribcage internal energy distribution of THUMS and VIVA+ respectively, in medium speed impacts. *Bottom left-right*: rib-cage internal energy distribution of THUMS and VIVA+ respectively, in high speed impacts.

Appendix E
Full-scale frontal sled test

Kinematics – comparison between THUMS and VIVA+.

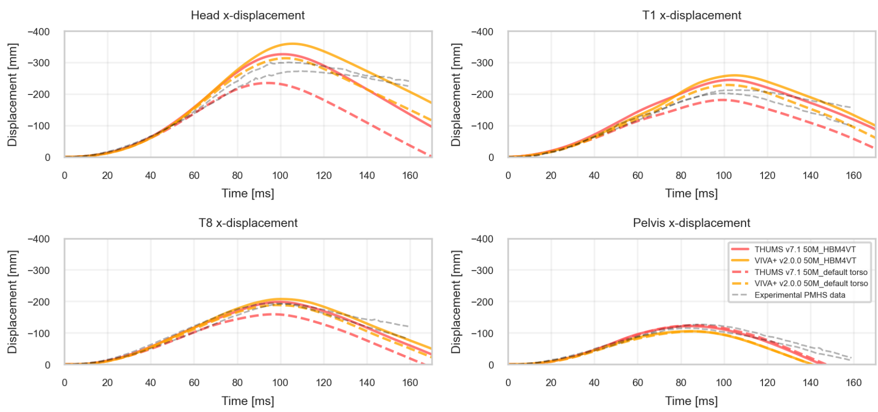

Fig. E1. Comparison of kinematic responses of THUMS and VIVA+ positioned based on HBM4VT set-up and the default torso posture, with PMHS data.

Ribcage internal energy distribution of THUMS in HBM4VT and default torso posture.

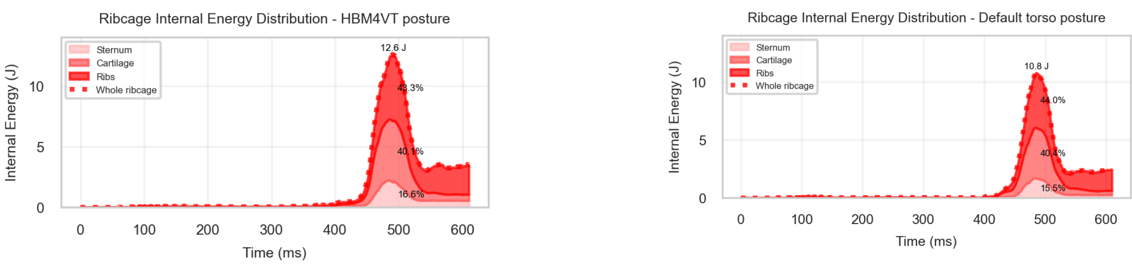

Fig. E2. Rib-cage internal energy distribution for the full-scale frontal sled test. *Left*: ribcage internal energy distribution of THUMS in HBM4VT posture. *Right*: rib-cage internal energy distribution of THUMS in default torso posture.

TABLE EI
KINEMATIC COMPARISON BETWEEN THUMS AND VIVA+ IN FRONTAL SLED TEST

Timeframe	THUMS	VIVA+
0 ms	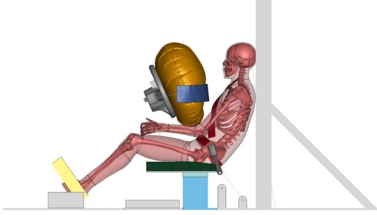	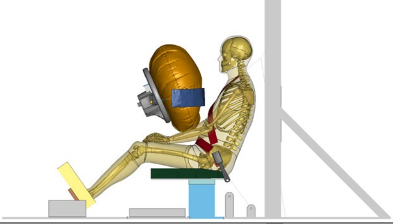
25 ms	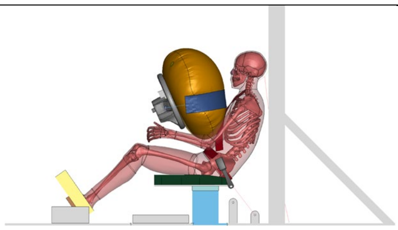	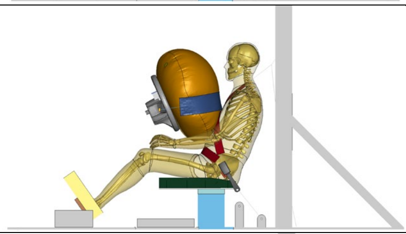
50 ms	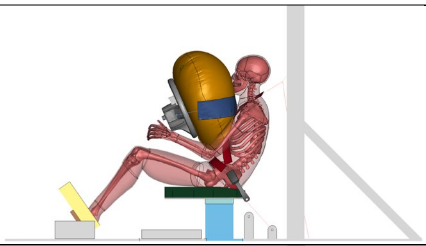	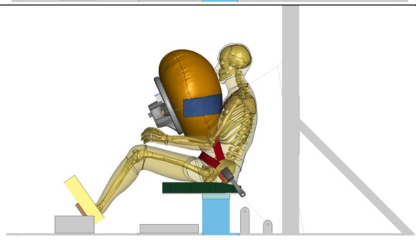
75 ms	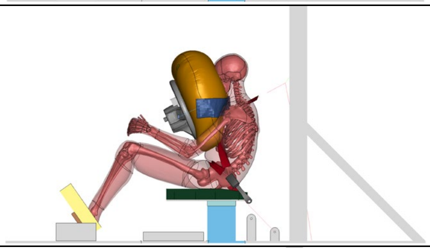	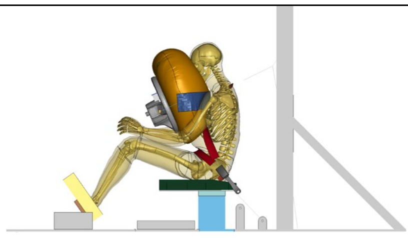
100 ms	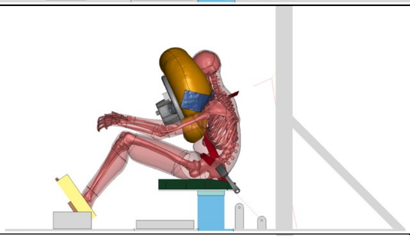	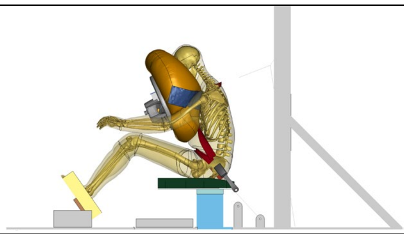
125 ms	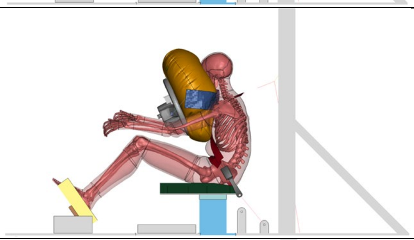	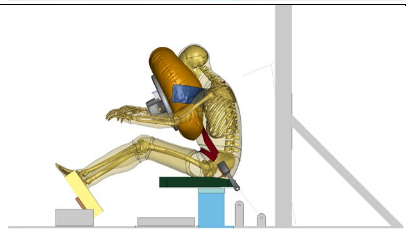
150 ms	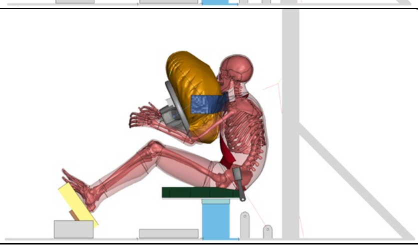	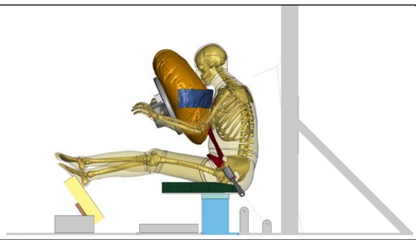

Appendix F
Individual rib fracture risk and MPS distribution of HBMs compared to the PMHS fracture sites

TABLE FI
RIB FRACTURE PREDICTION AND MPS DISTRIBUTION OF HBMs COMPARED TO PMHS FRACTURES

Loadcase	AGE	PMHS Fractured ribs/sites	MPS Distribution - THUMS	MPS Distribution – VIVA+	Individual rib fracture risk – THUMS & VIVA+
Denuded thorax compression – Upper thorax [19]	75	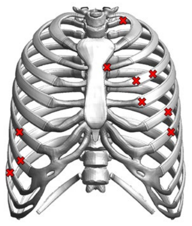	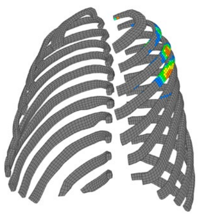	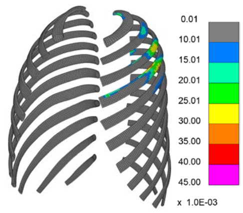	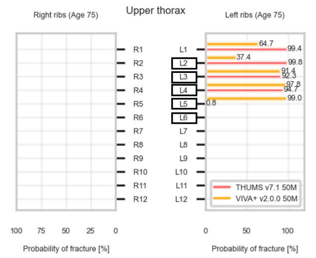
	48	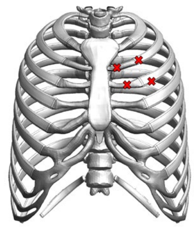			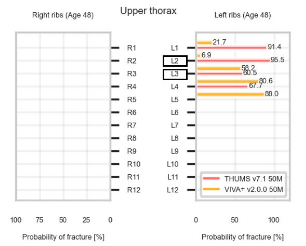
Denuded thorax compression-Mid thorax [19]	52	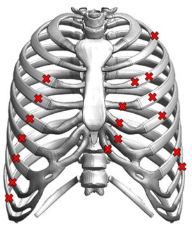	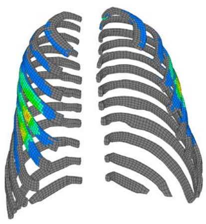	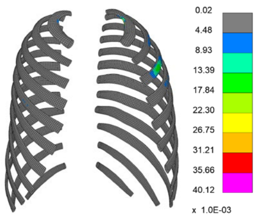	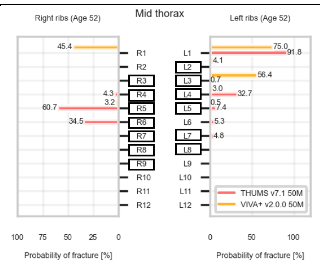
	67	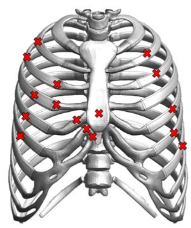			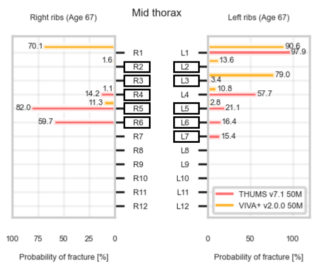
Denuded thorax compression-Lower thorax [19]	72	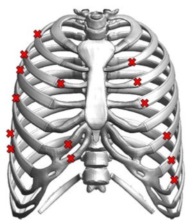	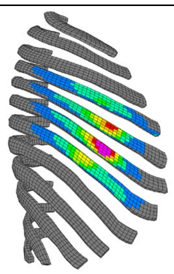	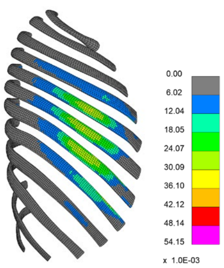	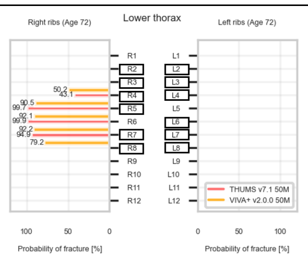
Lateral hub impact - Medium speed [22]	38	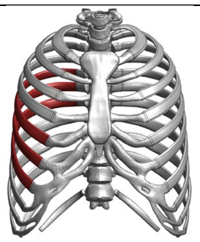	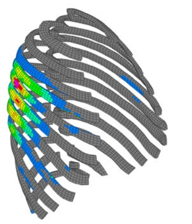	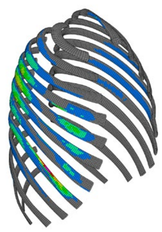	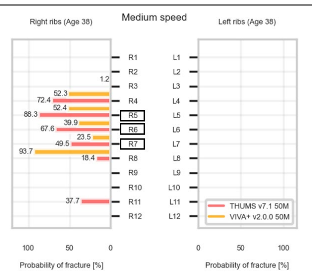

<table>
<tr><td rowspan="2">Lateral hub impact - Medium speed [22]</td><td>64</td><td>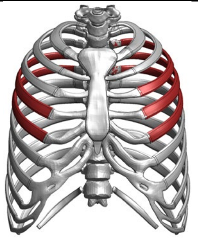</td><td rowspan="2">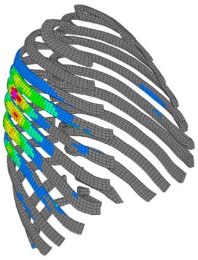</td><td rowspan="2">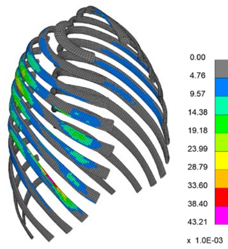</td><td>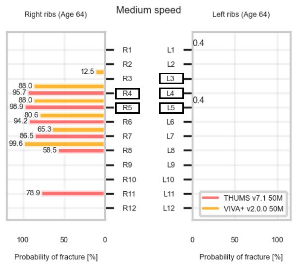</td></tr>
<tr><td>66</td><td>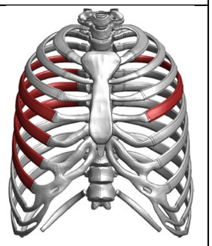</td><td>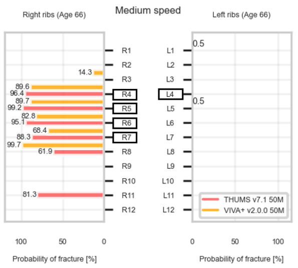</td></tr>
<tr><td rowspan="3">Lateral hub impact - High speed [22]</td><td>49</td><td>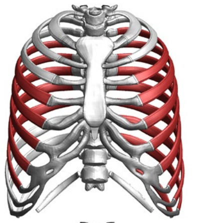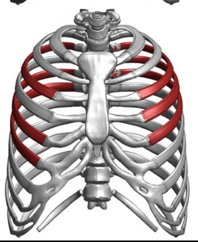</td><td>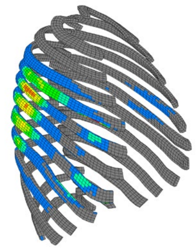</td><td>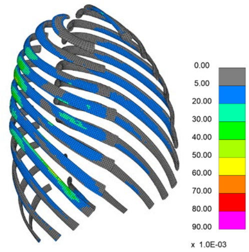</td><td>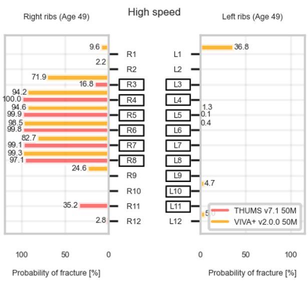</td></tr>
<tr><td>29</td><td>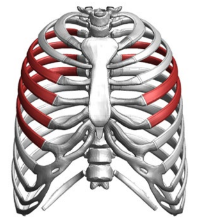</td><td rowspan="2">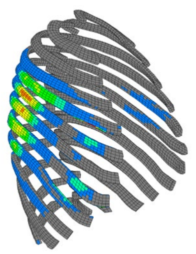</td><td rowspan="2">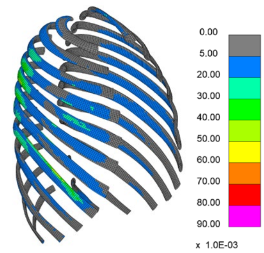</td><td>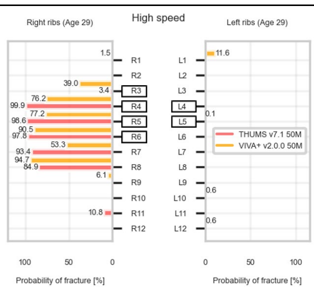</td></tr>
<tr><td>64</td><td>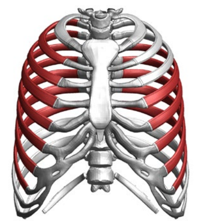</td><td>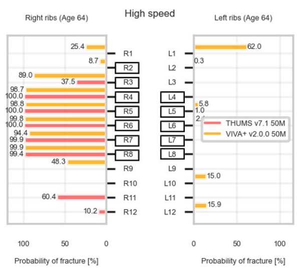</td></tr>
<tr><td>Frontal hub impact [21]</td><td>80</td><td>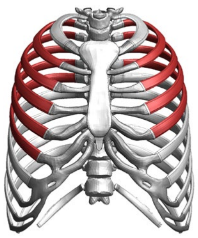</td><td></td><td></td><td>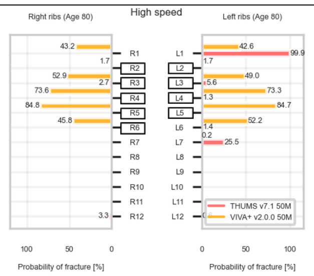</td></tr>
</table>

Frontal hub impact [21]	29	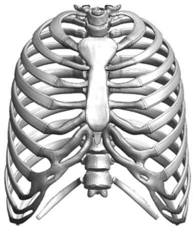	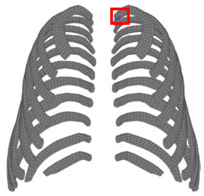	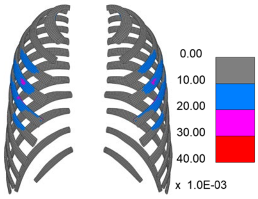	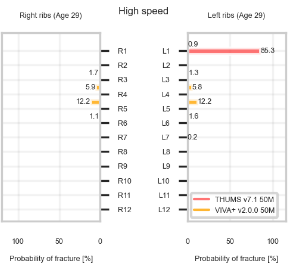
	72	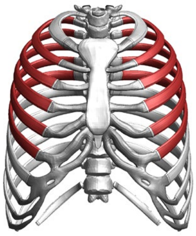			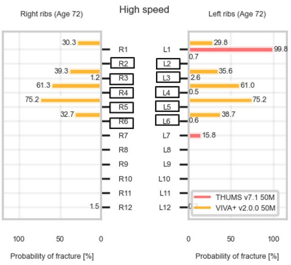
Full-scale frontal sled test [24]	68	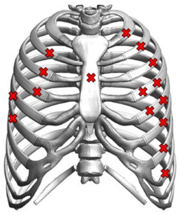	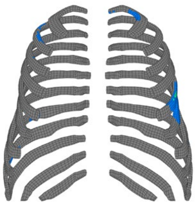	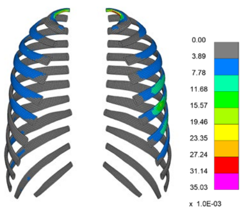	
	74	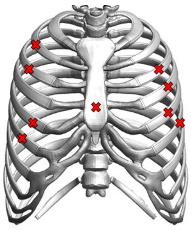 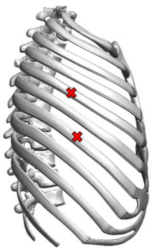	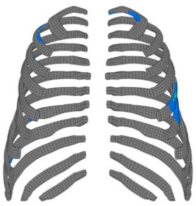 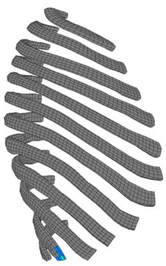 R11 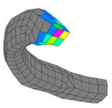	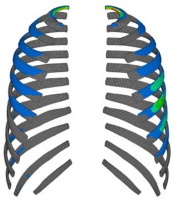 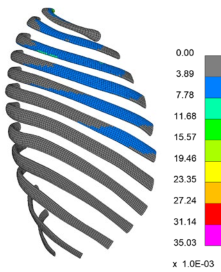 R1 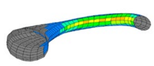	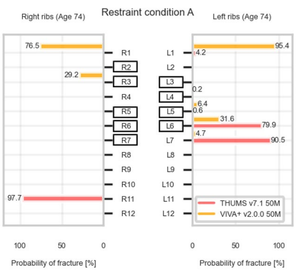

<table>
<tr><td>Full-scale frontal sled test [24]</td><td>94</td><td></td><td>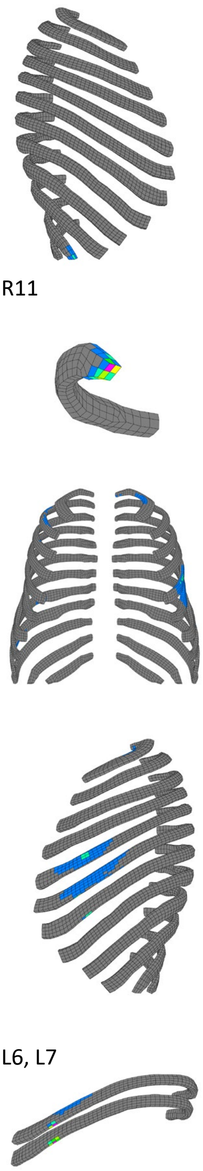</td><td>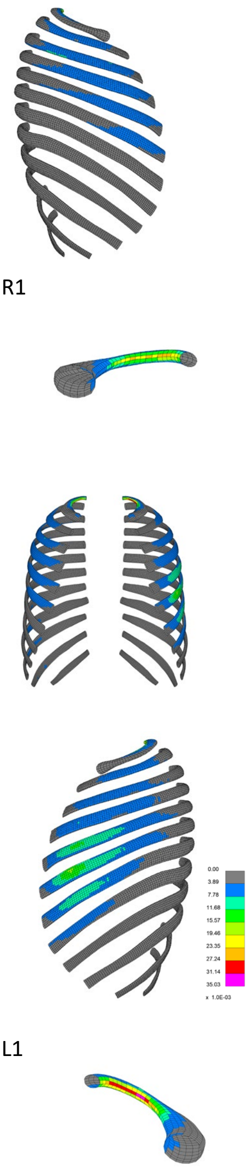</td><td>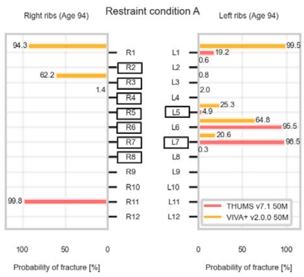</td></tr>
</table>

Appendix G

Statistical analyses of rib fracture risks – THUMS, VIVA+, and PMHS

NFR 3+ risks and prediction errors of THUMS and VIVA+ compared to PMHS in different loading conditions.

TABLE GI

LOAD CASES AND CORRESPONDING NFR 3+ RISKS AND PREDICTION ERRORS

Load case	**Impact type/Location/ Velocity**	**PMHS ID used in experiment**	**PMHS - AGE**	**PMHS – NFR 3+ risk**	**THUMS – NFR 3+ risk**	**THUMS – NFR 3+ risk “error”**	**VIVA+ – NFR 3+ risk**	**VIVA+ – NFR 3+ risk “error”**
Denuded thorax compression [19]	Upper thorax	Subject 2	75	1	0.99	-0.01	0.97	-0.03
		Subject 3	48	0	0.75	0.75	0.52	0.52
	Mid thorax	Subject 4	52	1	0.45	-0.55	0.04	-0.96
		Subject 5	67	1	0.86	-0.14	0.29	-0.71
	Lower thorax	Subject 1	72	1	0.97	-0.03	0.96	-0.04
Lateral hub impact [22]	Medium speed – 6.5 m/s	947	38	1	0.78	-0.22	0.29	-0.71
		RNY2	64	1	1.00	0.00	0.92	-0.08

		954	66	1	1.00	0.00	0.94	-0.06
	High speed – 9.5 m/s	863	49	1	1.00	0.00	1.00	0.00
		993	49	1	1.00	0.00	1.00	0.00
		986	29	1	1.00	0.00	0.92	0.08
		063	64	1	1.00	0.00	1.00	0.00
Frontal hub impact [21]	High speed – 6.7 m/s	15FM	80	1	0.04	-0.96	0.99	0.01
		20FM	29	0	0.00	0.00	0.00	0.00
		22FM	72	1	0.01	-0.99	0.94	-0.06
Full-scale frontal sled test [24]	Restraint condition A	PMHS 1	74	1	0.78	-0.28	0.45	-0.55
		PMHS 2	68	1	0.60	-0.40	0.30	-0.70
		PMHS 3	94	1	0.95	-0.05	0.91	-0.09

Under prediction | Correct prediction | Over prediction
-1.0 -0.1 0.1 1.0

Mean NFR 3+ prediction errors of THUMS and VIVA+ in different load cases.

TABLE GII
LOAD CASES AND CORRESPONDING NFR 3+ RISK MEAN PREDICTION ERRORS

Load case	Impact type/Location/Velocity	Mean NFR 3+ risk error - THUMS	Mean NFR 3+ risk error – VIVA+
Denuded thorax compression [19]	Upper thorax	0.37	0.24
	Mid thorax	-0.35	-0.84
	Lower thorax	-0.03	-0.04
Lateral hub impact [22]	Medium speed – 6.5 m/s	-0.07	-0.28
	High speed – 9.5 m/s	0.00	0.02
	Mean	-0.03	-0.13
Frontal hub impact [21]	High speed – 6.7 m/s	-0.65	-0.01
Full-scale frontal sled test [24]	Restraint condition A	-0.24	-0.44

Under prediction | Correct prediction | Over prediction
-1.0 -0.1 0.1 1.0

Brier score comparison between THUMS and VIVA+ in various load cases.

TABLE GIII
LOAD CASES AND CORRESPONDING BRIER SCORES

Load case	Impact type/Location/Velocity	Brier score – THUMS left ribs	Brier score – VIVA+ right ribs	Brier score – THUMS left ribs	Brier score – VIVA+ left ribs
Denuded thorax compression [19]	Upper thorax	0.12	0.12	0.18	0.18
	Mid thorax	0.35	0.51	0.47	0.42
	Lower thorax	0.36	0.26	0.5	0.5
Lateral hub impact [22]	Medium speed – 6.5 m/s	0.13	0.16	0.11	0.11
	High speed – 9.5 m/s	0.17	0.12	0.38	0.40
Frontal hub impact [21]	High speed – 6.7 m/s	0.27	0.1	0.32	0.1
Full-scale frontal sled test [24]	Restraint condition A	0.58	0.5	0.41	0.47

Brier score scale
0.0 0.1 0.2 0.3 0.5 1.0

Mean prediction error of individual ribs of THUMS and VIVA+ in various load cases.

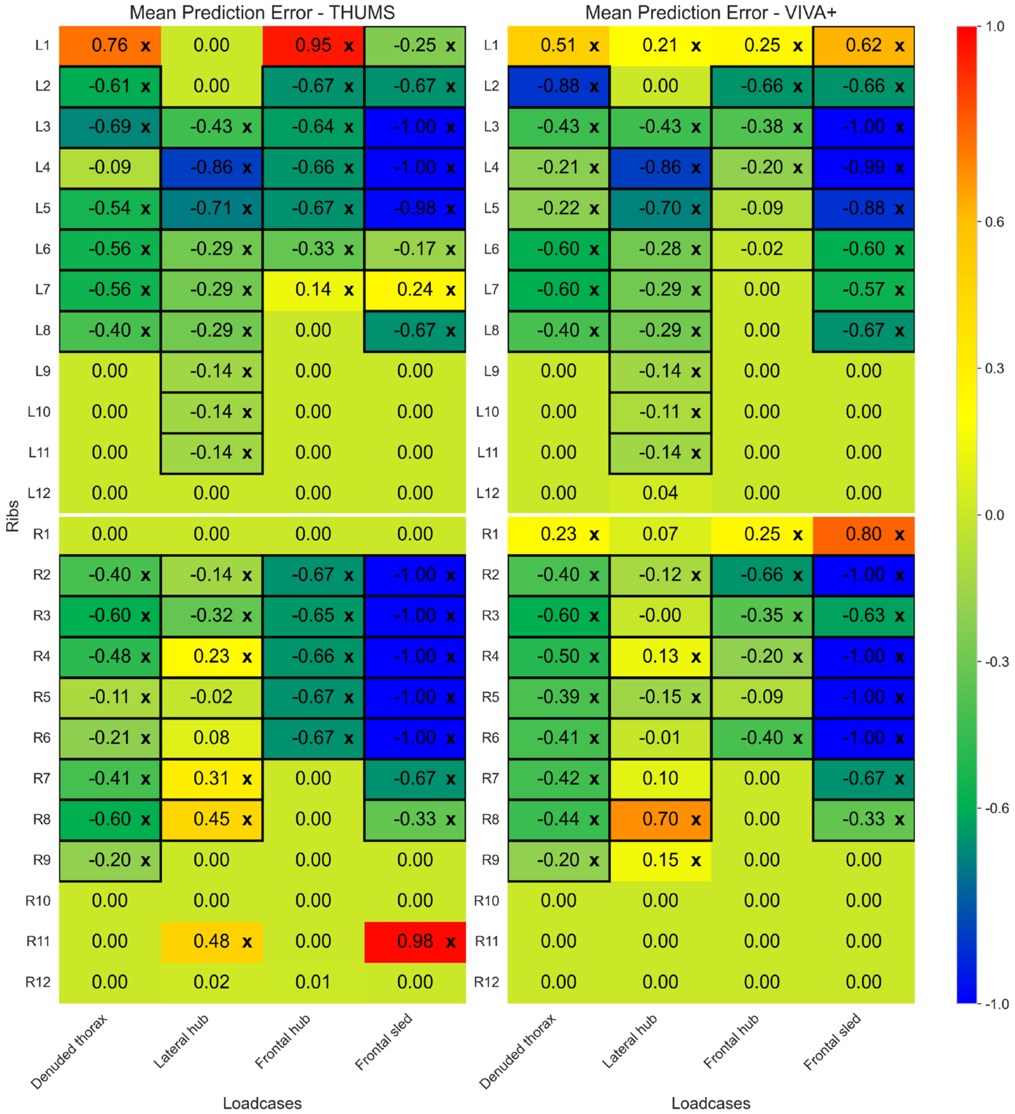

Fig. G1. Comparison of mean prediction errors of THUMS and VIVA+. Lower error values indicate a good prediction. Positive values show overprediction and negative values show underprediction. "x" marks indicate the ribs that exhibit poor prediction. Fractured ribs in PMHS are boxed in black.

Appendix H
Costal cartilage material and geometrical – THUMS & VIVA+

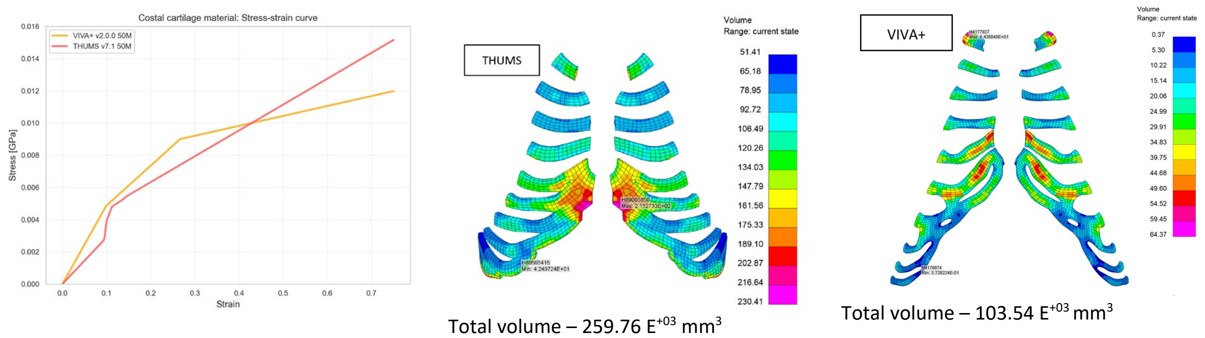

Fig. H1. Material and geometrical properties of costal cartilage. *Left*: Stress-strain curves of THUMS and VIVA+ costal cartilage material. *Middle*: Volume fringe plot of THUMS costal cartilage. *Right*: Volume fringe plot of VIVA+ costal cartilage.

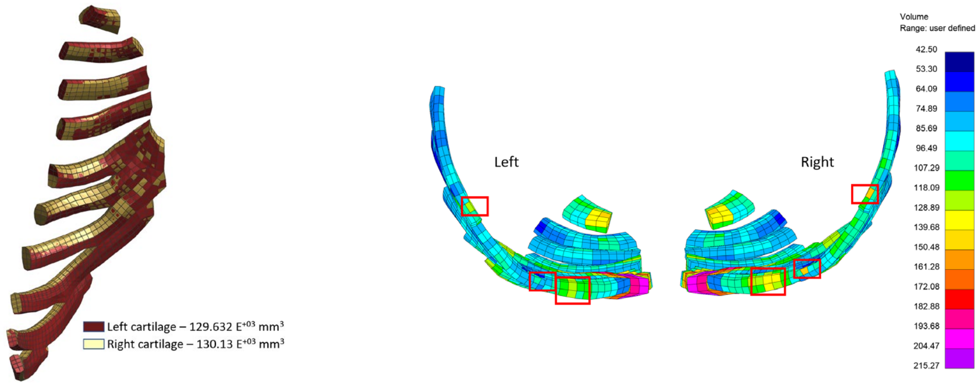

Fig. H2. Geometrical difference between THUMS left and right cartilage. *Left:* Overlay of the right cartilage on the left. *Right*: Volume fringe plot with examples of few solid elements with volume discrepancies (marked as red boxes).